Paper No.
11298

NACE INTERNATIONAL CORROSION 2011 CONFERENCE & EXPO

Mercury Embrittlement Crack Initiation in 5083 Aluminum Alloys – the Role of the Oxide Film

Richard E Clegg
Process Engineering and Light Metals Centre, CQUniversity Australia
Bryan Jordan Drive
Gladstone, QLD 4680
Australia

ABSTRACT

Mercury Embrittlement is a significant problem in natural gas facilities using aluminum cold boxes and has led to a number of major plant incidents. It has been postulated that the natural passive layer on aluminum provides an effective barrier between droplets of mercury and the underlying aluminum and this prevents mercury embrittlement. However, under certain circumstances this barrier is breached and embrittlement can occur. In this paper the condition of the mercury-aluminum interface is measured using ac impedance techniques and the effects of film aging conditions on the stability of the interface are studied. The film was modeled as a constant phase element and resistor in parallel and it was found that the resistance of the film increased with aging, although the effective film thickness only changed slightly. The paper finds that galvanic corrosion between the mercury droplet and underlying aluminum is likely to be a major cause of the breakdown of the mercury-aluminum interface.

Key words: Mercury embrittlement, aluminum, liquid metal embrittlement, gas processing

INTRODUCTION

Mercury embrittlement of aluminum cryogenic heat exchangers is an established problem in the gas industry and has been the cause of a number of industrial failures[1-6]. Many gas deposits contain small levels of mercury and this mercury can be liberated with the gas stream. During compression and preliminary separation, the gas is chilled and compressed until the heavier fractions of the gas are liquefied. During this process, it is possible for mercury to precipitate from the gas stream and accumulate in the cryogenic heat exchangers. Many cryogenic heat exchangers are made of 5083 aluminum and it is possible that liquid mercury can be present on the surface of these heat exchangers. Mercury is known to severely embrittle aluminum alloys and a number of failures have been recorded, including a major incident in South Australia in 2004[7].
In a recent study[8], the author has demonstrated that the oxide film that forms on aluminum in the atmosphere can act as a barrier to contact between mercury and the underlying metallic aluminum. This paper presents a study of the effects of surface roughness on the aluminum-mercury interface using impedance spectroscopy and examines the effect of exposure time on the interface impedance. The alloy investigated was aluminum alloy 5083, a commonly used alloy in heat exchanger construction in the gas processing industry. Impedance spectroscopy is used to measure the integrity of the film and to study the effects of some environmental parameters on the ability of the film to provide an effective barrier to the mercury. The interface can be described as an equivalent circuit similar in form

to that shown in Figure 1. The capacitance component (C_{eff}) of the equivalent circuit will give an indication of the average film thickness through the following equation.

$$d = \frac{A\varepsilon\varepsilon_0}{C_{eff}} \tag{1}$$

where d is the film thickness, A is the area of contact between the mercury and aluminum oxide film, ε_o is the permittivity of a vacuum and ε is the relative dielectric constant of the material. In this technique, the complex impedance of the mercury-aluminum cell is measured over a range of frequencies. At each frequency, the complex impedance, Z, was determined.

$$Z = Z' + jZ'' \tag{2}$$

Where Z' is the real component and Z'' is the imaginary component of the complex impedance and Z' and Z'' are plotted on a Nyquist plot which can be used to check the effectiveness of models for the interface and reactions taking place.

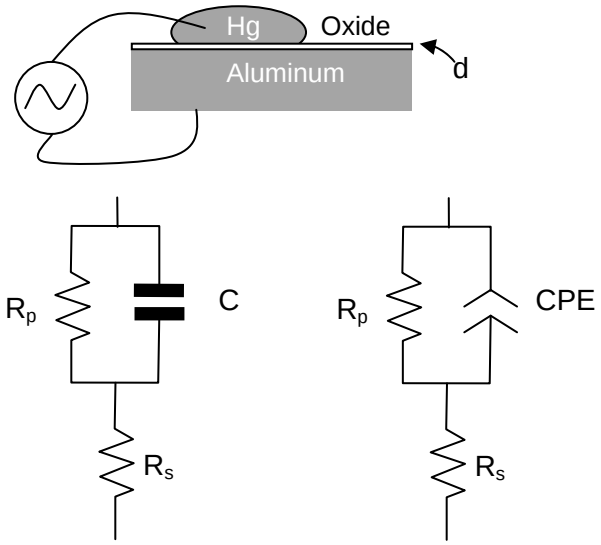

Figure 1 Schematic of the equivalent circuits used to investigate oxide film integrity.

The results have shown that in many instances, the impedance of the interface can be most effectively modeled using a constant phase element, rather than an ideal capacitor. A constant phase element (CPE) can be regarded as an imperfect capacitor, as shown in the right hand circuit in Figure 1. According to Hirschorn *et al.*[9], the electrical response of the circuit can be given by the following equation.

$$Z(\omega) = R_s + \frac{R_p}{1 + (j\omega)^{\alpha} QR_p} \tag{3}$$

where $Z(\omega)$ is the complex impedance at a frequency of ω, Q and α are CPE parameters that are independent of frequency. If it is assumed that the effective capacitance is a result of variations in the film properties normal to the surface, from Hirschorn *et al.*[9] the effective capacitance can be given by the following equation.

$$C_{eff} = Q^{1/\alpha}.R_p^{\frac{(1-\alpha)}{\alpha}} \tag{4}$$

EXPERIMENTAL PROCEDURE

Oxide file measurements were carried out using plate samples of Al 5083-H116/321. Samples were ground using metallographic grinding papers to produce surfaces with different roughness. Five surface preparation treatments were used: P60, P120, P240, P600 and polished to 1 μm diamond finish. The surfaces were then aged artificially in a 100% humid environment for 47 hours in order to develop an oxide film. Representative surfaces were examined using an optical microscope and using a JEOL JSM 6360 LA scanning electron microscope. The microscope was used in secondary electron mode with an accelerating voltage of 15kV. Stereopairs of the surface were taken at appropriate magnifications and 3-D surface reconstruction was carried out using MEX 3.0 software from Alicona[10], which was able to determine the surface roughness parameters. In the case of oriented surfaces (i.e. the ground surfaces), the surface roughness was measured perpendicular to the direction of the grinding marks. For the sample polished to 1 micron diamond, the surface features were randomly oriented and so surface roughness was not directional. In all cases, the ratio of true surface area to projected area was determined using the MEX software and this ratio was used to estimate the true surface area of contact between the aluminum and mercury.

Table 1 Surface roughness data for the samples tested.

Grinding condition	R_a (μm)	True area/ projected area
P60	1.98	1.24
P120	1.56	1.30
P240	0.835	1.25
P600	0.552	1.24
Polished to 1 μm diamond	0.057	1.01

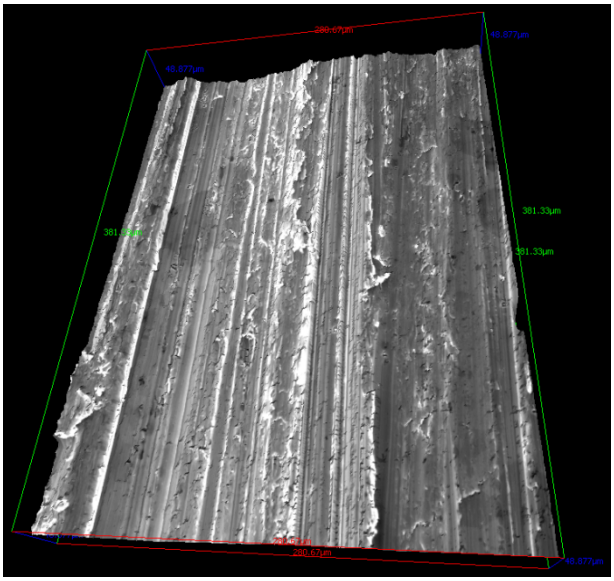

Figure 2 Three dimensional reconstruction of a ground surface using MEX.

Prior to testing, a mercury droplet was placed on the surface of the aluminum samples such that a contact area of approximately 5 mm diameter was maintained. Electrical contact was made on the aluminum via metallic clips and in the mercury through a 0.1mm diameter platinum wire. The impedance of the interface was measured using a Solartron 1260 frequency response analyzer in stand-alone mode and Zplot software. Once testing was completed, the mercury droplet was weighed to an accuracy of 0.0001 gm. A previously determined calibration curve relating weight of mercury

droplet to projected area of the droplet was used to convert the weights into approximate area of contact. Once the projected area was estimated the true area of contact was estimated using the true area to projected area ratios determined using the MEX software. These ratios were typically 1.3 for the ground surfaces and close to 1 for the polished surface. All tests were carried out at room temperature in an air conditioned room (23°C).

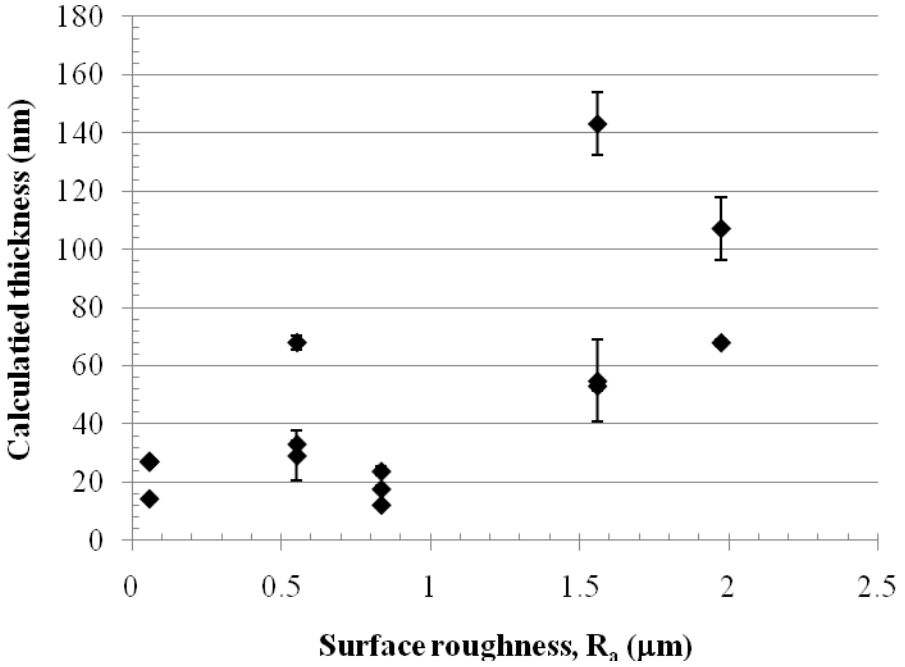

Figure 3 Effect of surface roughness on estimated oxide film thickness.

In order to study the interface between the mercury and aluminum the following test protocol was used. Three spots on the surface of the aluminum were tested for each surface roughness. The mercury droplets were placed on the aluminum surface on an area not to be tested and then were rolled onto the test area. This was done to minimize any damage to the film caused by the mercury dropping onto the surface. Immediately after the droplet was rolled onto the surface, the complex impedance of the interface was measured using a 20 mV amplitude and a frequency range from 100 kHz to 1 Hz. This was repeated five times to give a total of six frequency sweeps for each position. Each sweep took approximately 1 minute and they followed on each other without a break.

In most cases, the Nyquist plots involved the development of a typical R-C-R type response, as expected for the circuit shown in Figure 1 although the capacitor element replaced a constant phase element, as shown in the right hand circuit. In general, R_s was small and typically of the order of 1Ω or less and represents the resistance of the circuit outside of the mercury-aluminum interface. The values of R_s, Q, α and R_p were determined by curve fitting the impedance data using Zplot. The equivalent thickness of the film was calculated on the basis of the effective capacitance determined using eqn.4. It was assumed that the dielectric constant of the film material was equivalent to that of alumina (approx.9.8). In the calculations, the contact area was calculated by multiplying the projected contact area by the true area to projected area ratio shown in Table 1.

A series of time studies were carried out in which samples of polished aluminum which had been aged for one month in dry air were exposed to mercury droplets for a period of time in laboratory air. During this period the complex impedance of the interface was measured at 2 s intervals at a frequency of 10 Hz. From these studies, the magnitude of the complex impedance and the phase angle were plotted with respect to time. Also the results were examined on the complex Z'/Z" plane for features controlling the degradation of the interface.

RESULTS

Once prepared, representative samples of the prepared surfaces were examined to characterize the surface. Figure 2 shows an SEM image of the surface ground to P120. Stereoimages of the surfaces were taken at magnifications suitable to the surface roughness being measured at angles of 0 and ±5 degrees. Although a significant number of surface roughness parameters were measured, only R_a and the ratio of the true surface area to projected surface area is reported here. These are shown in Table 1.

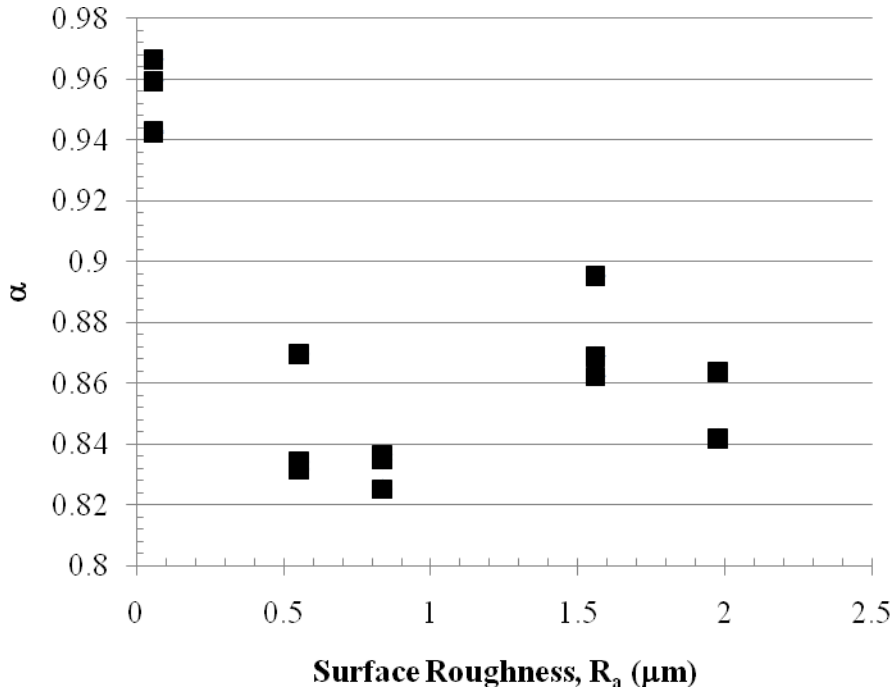

Figure 4 of surface roughness on the constant phase element component,α as per eqn.3.

Figure 3, Figure 4 and Figure 5 show the effects of surface roughness on the interface parameters. Figure 3 shows that as the surface roughness increases, the effective film thickness increases from 20 nm to approximately 100 nm. The degree of scatter also increases. At the same time, Figure 4 shows that α decreases. α is a measure of how close to an ideal capacitor the film is. If $\alpha = 1$, then the constant phase element behaves as an ideal capacitor whereas if $\alpha = 0$, the capacitor behaves as an ideal resistor. As can be seen, for low surface roughness, α is close to 1. As the surface roughness increases this decreases, suggesting that the film becomes more complex. Figure 5 shows the effect of the surface roughness on the interface resistance normalized with respect to the area of contact and shows that the interface resistance increase several orders of magnitude as the surface roughness increased. It was also notable that the degree of scatter in the results also increased as the surface roughness increased.

The effect of time of exposure of the aluminum to a mercury droplet is as shown in Figure 6 and Figure 7. As can be seen the complex impedance decreases over time, with a number of abrupt drops. At the same time the phase angle tends towards zero. Figure 6 and Figure 7 are typical of a number of similar graphs obtained for time effects on the interface. In addition, a number of frequency sweeps were measured during these experiments. It was found that during aging, the film thickness did not change significantly in these tests. However, R_p changed significantly. Modeling of the complex interface using eqn.3 indicated that the form of Figure 6 could best be replicated if the change in interfacial behavior was due to gradual degradation of R_p, with the other parameters remaining constant. This suggests that the degradation of the interface shown in Figure 7 is largely due to degradation of R_p.

DISCUSSION

Although mercury embrittlement of aluminum has been studied previously, the role of the oxide film has not been fully understood. Previous attempts at measuring the interface through impedance techniques have suffered from experimental difficulties, although recent studies by the author have shown that the impedance results can give useful information about the mercury/aluminum interface and are strongly influenced by the formation of the oxide film on the surface of the aluminum. It is clear also from this work that the surface roughness of the material can affect the impedance results. The results shown in Figure 3, Figure 4 and Figure 5 suggest that the interface between the mercury and aluminum increased in thickness and resistance with surface roughness and became more complex, as indicated in the changes in α. However, the experimental design was such that all of the surfaces were aged under the same conditions after bare metal was formed. Each of the surfaces would have had slightly different degrees of plastic deformation and this may have affected the way in which the aluminum surface oxidized. However, it is believed that this would have been a secondary effect on the growth of oxide films and it was expected that similar types of oxide film would have formed on each of the samples. Furthermore, the thickness of the oxide films on polished material was measured at approximately 20nm. This is significantly smaller than the surface roughness of all of the surfaces studied here except for the polished sample. It is proposed, therefore, that the rough surfaces would have had an oxide film of a similar value, albeit over a rough surface. Hence the changes in impedance parameters with surface roughness may be better explained by a mechanism other than simply an increase in the oxide film thickness with surface roughness.

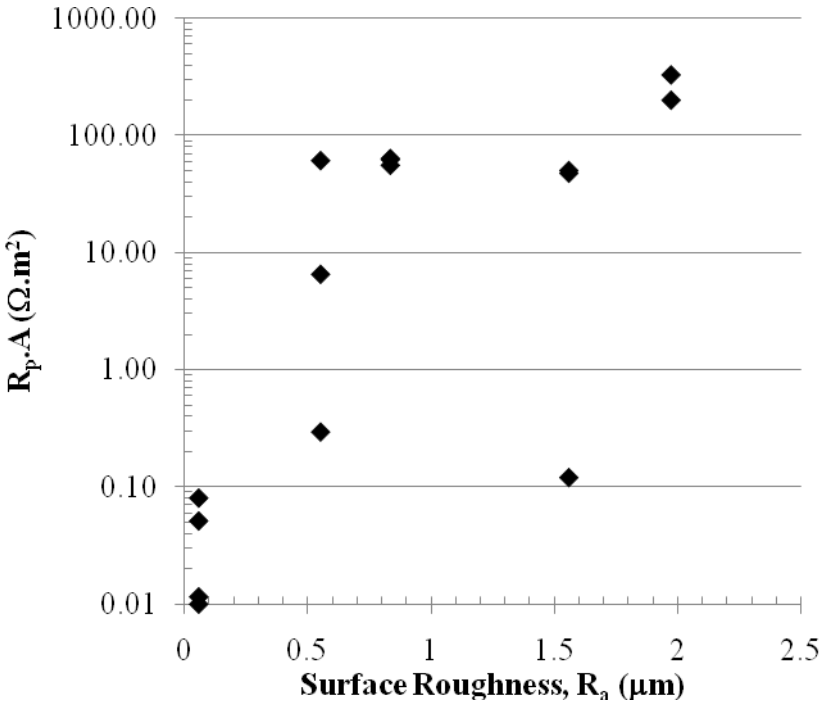

Figure 5 Effect of surface roughness on the normalized parallel resistance of the interface.

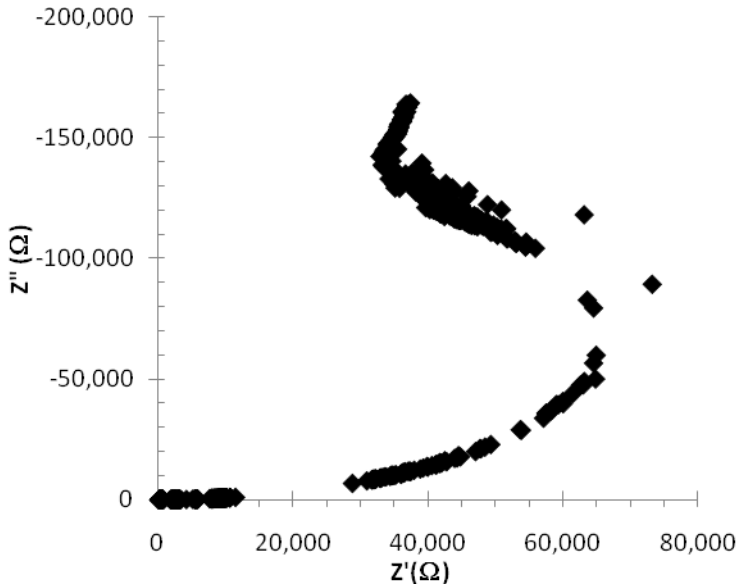

Figure 6 Nyquist plot for time dependent degradation of the interface. Measurements were taken over 27 hrs at 2 sec intervals. Impedance was measured using a voltage amplitude of 20 mV and a frequency of 10 Hz.

Mercury has a high surface tension. As a result, it is likely that it will not fill the entire rough surface and the droplets may bridge over rough areas. Furthermore, although the surfaces were cleaned and dried with alcohol after aging, moisture may have become trapped in the rough surfaces during the aging process. This moisture may have helped separate the mercury and aluminum. Good contact between the mercury and aluminum oxide film may only be occurring at asperities on the surface. This model would explain the observed phenomena, as the effective area of contact between the droplet and the aluminum would be significantly reduced.

If this asperity model is correct, it masks somewhat the issue that the actual resistance normalized for area of the interface at the asperities may be quite small and that the higher resistance of the higher surface roughness specimens may be a result of lower actual contact area between the mercury and aluminum. On the polished samples, the normalized resistance of the interface was as low as $0.01\Omega.m^2$. This implies that significant current can be passed through the interface. Mercury and aluminum have a significant difference in electronegativity (approximately 1 V at standard conditions). This indicates that a galvanic couple may be set up between the mercury and aluminum and this may lead to accelerated corrosion of the aluminum. Laboratory observations have shown that if mercury droplets are permitted to sit on aluminum in laboratory atmospheres for an extended period of time, the interface between the mercury and aluminum will break down and spontaneous wetting of the aluminum will occur. Once this occurs, rapid corrosion of the aluminum follows, catalyzed by the mercury. If the aluminum is stressed, then mercury embrittlement of the aluminum may proceed. Whether or not this is likely to occur depends on a number of factors. Increasing the oxide film thickness either through natural oxidation or by artificial means, will tend to increase the resistance of the interface to the extent that the resistance is high and this is known to improve the resistance to mercury embrittlement[11]. Under these circumstances, little current can pass through the interface and the corrosion of the galvanic couple will be slowed. Furthermore, in cryogenic gas compression units, the temperature is low and the conditions for corrosion may not be favorable. As a result, the ability of the galvanic couple to drive corrosion may not be significant. Although higher surface roughness may produce an apparently greater resistance at the interface, if the asperity model is correct, then areas of the interface may permit locally high currents and allow for galvanic corrosion to occur. Therefore, high surface roughness may not be an effective barrier to the degradation of the aluminum-mercury interface.

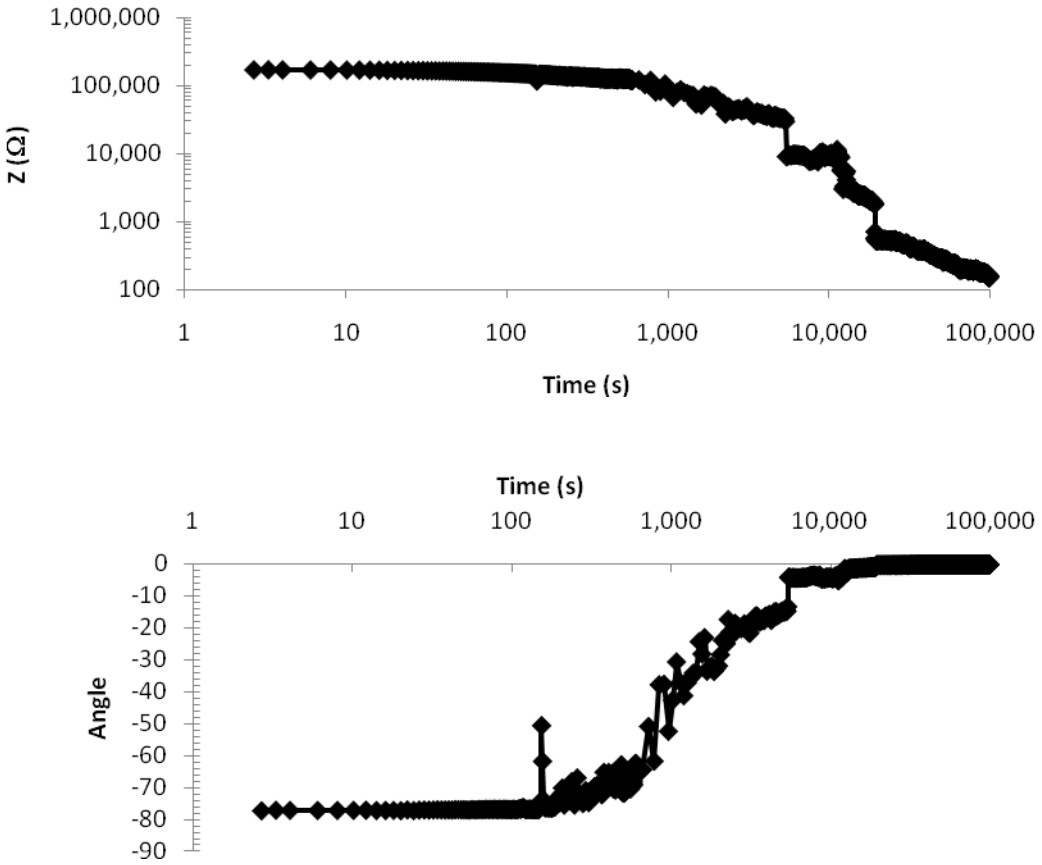

Figure 7 Effect of time of exposure on the impedance of the interface. The top graph is the absolute value of the impedance and the bottom graph is the phase angle.

The time series results show that as the film is exposed to the mercury in laboratory atmosphere, the film impedance degrades. Modeling of eqn.3 with respect to the experimental results suggests that this can largely be explained as being a result of degradation of R_p. The capacitive elements in the interface remain the same, suggesting that the film thickness is not significantly affected by the exposure to the mercury.

A degradation of R_p can result from a number of factors. One is that the resistance of the film can degrade over time, with an increasing number of charge carriers becoming available. A second mechanism is that oxidation of the aluminum occurs, particularly around the edges of the droplet of mercury, and this causes the film in this region to gradually break down. This can be seen in Figure 8, which shows the surface of aluminum once a mercury droplet has been removed. The arrows show the edge of the mercury droplet, which has been delineated by a corrosion mark. Slightly inside the ring of the droplet is a region where accelerated corrosion of the aluminum has occurred due to wetting of the aluminum by the mercury. This is suggesting that the wetting process may occur from reactions that occur at the interface between the mercury droplet, the aluminum and the atmosphere.

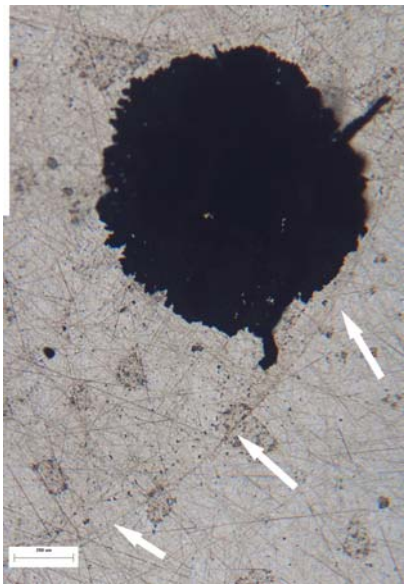

Figure 8 Surface of the aluminum showing the edge of where a mercury droplet had been (arrowed). The large dark droplet is an area where accelerated corrosion had occurred as a result of amalgamation between the mercury and aluminium.

CONCLUSIONS

Increases in surface roughness of Al5083 lead to apparent increases in the thickness and resistance of the interface between droplets of mercury and the aluminum substrate. Furthermore, the interface became more complex as the surface roughness increased, as evidenced by the changes in α. These observations were attributed to incomplete contact between the aluminum passive film and the mercury, with complete contact only occurring at asperities on the surface. Increases in surface roughness may not provide an effective barrier to galvanic corrosion driven by electrochemical differences between the aluminum and the mercury, as it is considered likely that the resistance normalized with respect to area would remain low and localized galvanic corrosion effects may occur. The effect of long term exposure of aluminum to mercury droplets appears to be the gradual degradation of the impedance of the interface and was manifested as a change in R_p. This was attributed to corrosion at the interface between the mercury droplet, the aluminum and the atmosphere, which caused a localized breakdown of the film.

ACKNOWLEDGEMENTS

The author wishes to acknowledge the support of Dr.Alan McLeod for his useful comments and discussion.

REFERENCES

[1] R.N. Bell, "Understanding and Preventing Failure of Aluminum Equipment in the Presence of Liquid Mercury", in: *Spring Meeting of the American Institute of Chemical Engineers*, AIChE, Atlanta, GA, 2005.
[2] M.D. Bingham, "Field detection and implications of mercury in natural gas", *SPE Prod.Eng.*, 5 (1990): 120-124.
[3] R. Coade, D. Coldham, "The interaction of mercury and aluminium in heat exchangers in a natural gas plants", *International Journal of Pressure Vessels and Piping*, 83 (2006): 336-342.
[4] D.R. Nelson, "Mercury attack of brazed aluminum heat exchangers in cryogenic gas service", in: *73rd Annual GPA Convention*, New Orleans, Louisiana, 1994, pp. 178-183.

[5] S.M. Wilhelm, "Risk Analysis for Operation of Aluminium Heat Exchangers Contaminated by Mercury", *Process Safety Progress*, 28 (2008): 259-266.
[6] S.M. Wilhelm, N. Bloom, "Mercury in petroleum", *Fuel Proc.Tech.*, 63 (2000): 1-27.
[7] P.L.J. Fernandes, R.E. Clegg, D.R.H. Jones, "Failure by liquid metal induced embrittlement ", *Eng.Fail.Anal.*, 1 (1994): 51-63.
[8] R.E. Clegg, "Measurements of the interface between 5083 aluminium and liquid mercury using impedance spectroscopy", *Corr.Sci.*, 52 (2010): 4028-4034.
[9] B. Hirschorn, M.E. Orazem, B. Tribollet, V. Vivier, I. Frateur, M. Musiani, "Determination of effective capacitance and film thickness from constant-phase-element parameters", *Electrochimica Acta*, (2009).
[10] alicona, "MeX", in, www.alicona.com, 2005.
[11] B. Bavarian, "Liquid metal embrittlement (LME) of the 6061 Al-alloy by mercury ", in: *Corrosion 2004*, NACE, New Orleans, LA, 2004.